



# Reduction of Speed Ripple in BLDC Motor Aimed at using in the Servomotor of Aircraft Flap

Mohammadreza Soltanpour<sup>1\*</sup>, Hamid Radmanesh<sup>2</sup>, Reza Sobhani<sup>3</sup>

<sup>1,2</sup> Department of Electrical Engineering, Shahid Sattari Aeronautical University of Science and Technology, Tehran, Iran

<sup>3</sup> Faculty of Electrical and Computer Engineering, Babol Noshirvani University of Technology, Babol, Iran  
soltanpour@ssau.ac.ir

---

## Abstract

Drivers of brushless direct current motor (BLDC) are widely used for industrial servo applications, including servo motors used in aircraft flaps, where torque smoothness is a key requirement. One disadvantage of torque pulses, however, is the pulsation that causes the speed to fluctuate, which affects the performance of the drive, especially at low speeds and sensitive applications. In this research, to reduce these speed ripples, the iterative learning method (ILC) is presented. Although in brushless direct current motors, a conventional proportional-integral (PI) speed controller suppresses the speed ripples to some extent, the use of this controller alone is not sufficient for many high-performance applications. The simulations showed that utilizing the proposed control to the driver of BLDC motor could well reduce the motor speed ripple.

Keywords: Brushless direct current motor, Iterative learning control, Speed ripple, Flap, Servo motor

Article history: Received 10-Jan-2020; Revised 07-Feb-2021; Accepted 15-Feb-2021.

© 2020 IAUCTB-IJSEE Science. All rights reserved

---

## 1. Introduction

Brushless direct current motors (BLDCs) are widely used compared to induction motors and permanent magnet synchronous motors (PMSM) due to their high efficiency, power density and high torque to inertia ratio, make them a suitable choice for variable speed drive applications. The main disadvantage of BLDCs is the presence of pulsed torque and the torque ripple that periodically causes the ripple in position and the rotor speed. In any aircraft, the flaps play an important role in the way it flies. Any fixed-wing aircraft has flaps mounted on the trailing edges of the plane's wing. These are high-lift equipment that, at a certain airspeed, can actually increase the lift force of the aircraft's wing [1]. They serve various other purposes as well, including providing extra lift when the plane is taking off and increasing the curvature of the wing when they are extended, which allows the aircraft to generate the right amount of lift even at lower speeds. Flaps' movement in the aircraft wing is controlled by servomotor that uses brushless direct current motors. One of the important points in using flaps is that they should have as much softness in

movements as possible which ultimately increases the efficiency and performance of this equipment. Speed fluctuations, especially in high-precision applications, severely limit servo motor's performance. Also, these fluctuations in speed and torque cause undesirable mechanical vibration at the load side. Through increasing popularity of BLDCs in industrial applications, in recent years, much attention has been paid to reducing pulsating torques. In general, these techniques can be divided into two groups: the first one is by improving motor design make the reduction of the impulse torque, and the second technique for minimizing pulsating torque is based on active control schemes which modify the excitation of motor [2]. In terms of motor design, the deflection of the rotor magnets, the proper distribution of the winding, and other motor design features reduce torque ripple to some extent but do not completely eliminate it [3]. In addition, special machine design techniques increase the complexity of the production process, which leads to higher machine costs. The second technique, which is the focus of this paper, utilizes an additional

control to compensate the periodical torque pulses. In [4] and [5] a programmed stator current control is proposed to eliminate the harmonic components of the torque. However, in such a method, sufficient and accurate information of BLDC parameters, especially torque wave characteristics, is required, and also due to the open-loop control, a small error or changes in the parameters can lead to an increase in the motor torque ripple. Given the inherent limitations of open-loop control schemes, alternative methods using closed-loop control algorithms with online estimation techniques (e.g., a self-starting scheme [6] and an adaptive control algorithm [7]) to achieve the minimum pulsating torque is suggested. These control schemes are implemented in real time, either in speed or current (torque) loops. In torque control schemes, a known method of torque adjustment is to use online estimated torque based on electrical subsystem variables (current and voltage). Various algorithms for estimating instantaneous torque are presented in [8] to [11]. In [12] a robust ILC scheme is proposed that uses a sliding mode control (SMC) method to further reduce torque ripple and also diminish the disruption of the servomotor. In [13], a Lyapunov-based control model for torque prediction control of a permanent magnet synchronous machine (PMSM) is proposed. In this scheme, a cost function is introduced with respect to torque error, maximum torque per ampere (MTPA), and driver current limitation. Authors in [14] present a method for reducing torque, acoustic noise, and vibration in three-phase permanent magnet (PM) motors. In this scheme, a compensator is added to the q axis to minimize speed ripple. In [15] a combination of Model Predictive Control (MPC) and Iterative Learning Control (ILC) to increase the speed of system response and reduce ripple speed. The MPC through feedback updates the predictive model in real time and evaluates the output signal and control of the system according to cost.

In this paper, iterative learning control schemes that has been implemented in the time domain is presented with the aim of minimizing the speed ripples caused by torque pulses. Regardless of the differences in their control structures, both control schemes have the same drive configuration. Proposed control scheme is applied with the traditional PI speed controller, which provides the main reference current. In the steady state, the proposed controller generates compensating current that is used with the reference current to minimize the speed ripple. In order to evaluate the performance of ILC control scheme, the proposed scheme is modeled in Matlab/Simulink. The results showed an improvement in the steady state speed response of the BLDC motor, which indicates the effectiveness of the proposed ILC scheme. This

strategy can effectively reduce the ripple of speed waves.

## 2. BLDC Motor Modelling

By assuming that the BLDC motor is not saturated and also the eddy currents and residual losses are negligible, the stator voltage equations along the d, and q axis of the synchronous rotating reference frame are expressed as follows:

$$\frac{di_d}{dt} = -\frac{R}{L_d} i_d + \frac{L_q}{L_d} \omega_e i_q + \frac{1}{L_d} V_d \quad (1)$$

$$\frac{di_q}{dt} = -\frac{R}{L_q} i_q + \frac{L_d}{L_q} \omega_e i_d + \frac{1}{L_q} V_q \quad (2)$$

where  $i_{ds}$  and  $i_{qs}$  are the synchronous stator currents along the d and q axis, respectively.

In (1) and (2),  $L_d$  and  $L_q$  are the d and q axis stator inductance, respectively. Also,  $\omega_e$  denotes the electrical angular velocity, and  $R$  the stator resistance. It should be noted that  $L_d$  and  $L_q$  are equal. Due to the fact that the motor is controlled by the vector control method, the current  $i_{ds}$  is controlled at zero to obtain the maximum torque. As a result, the amount of output torque is expressed as follows:

$$T_m = \frac{3}{2} \frac{P}{2} \psi_{dm} i_{qs} = k_t i_{qs} \quad (3)$$

where  $k_t$  denotes torque constant and  $P$  the number of pole pairs. The dynamic equation of the motor is shown below:

$$\frac{d\omega_m}{dt} = -\frac{B}{J} \omega_m + \frac{k_t}{J} i_{qs} - \frac{T_l}{J} \quad (4)$$

where  $\omega_m$ ,  $T_l$ ,  $B$ , and  $J$  are respectively rotor mechanical speed, load torque, friction coefficient, and total motor inertia.

## 3. Pulsating Torque Analysis

### A) Flux Harmonics

Due to the distribution of non-sinusoidal flux density in the air gap, the resulting flux between the permanent magnet and the stator current in the abc frame includes 5<sup>th</sup>, 7<sup>th</sup>, 11<sup>th</sup>, etc. harmonics (multiples of the third harmonic do not exist in stator windings that have a star connection) [10]. In the synchronous rotating frame, the flux harmonics appear as a multiples of sixth harmonic.

$$\psi_{dm} = \psi_{d0} + \psi_{d6} \cos 6\theta_e + \psi_{d12} \cos 12\theta_e + \dots \quad (5)$$

### B) Current Offset Error

Dc offset in stator current measurement can lead to torque pulsation [13]. The stator currents are converted to voltage signals by current sensors and then digitally converted by analog-to-digital (A / D) converters. Unbalanced dc supply voltage in current sensors and inherent offsets of analog electronic elements cause dc offset. If it is assumed that the offset values of the current phases a and b are  $\Delta i_{as}$  and  $\Delta i_{bs}$  respectively, then the measured current along the q-axis is written as follows:

$$i_{qz-AD} = i_{qz} + \Delta i_{qz} \quad (6)$$

$$\Delta i_{qz} = \frac{2}{\sqrt{3}} \cos(\theta_s + \alpha) \sqrt{\Delta i_{as}^2 + \Delta i_{as} \Delta i_{bs} + \Delta i_{bs}^2} \quad (7)$$

where  $\alpha$  is a fixed-angular displacement and depends on  $\Delta i_{as}$  and  $\Delta i_{bs}$ . It is assumed that  $\theta_e = 2\pi f_s t$  is the base oscillation of the electric current and the current follows the reference current exactly. Then the motor current is displayed as follows:

$$i_{qz} = i_{qz-AD} - \Delta i_{qz} = i_{qz}^* - \Delta i_{qz} \quad (8)$$

Using equations (3) and (8), the mechanical torque is calculated as follows:

$$T_m = k_t (i_{qz}^* - \Delta i_{qz}) = T_m^* - \Delta T_{m,1} \quad (9)$$

By placing equation (8) in equation (9),  $\Delta T_m$  is obtained as follows:

$$\Delta i_{qz} = k_t \frac{2}{\sqrt{3}} \cos(\theta_s + \alpha) \sqrt{\Delta i_{as}^2 + \Delta i_{as} \Delta i_{bs} + \Delta i_{bs}^2} \quad (10)$$

Equation (10) shows that the offset in the current measurement causes a torque fluctuation at the fundamental frequency.

### C) Current scaling error

The output of the current sensor must be proportional to the input of the analog-to-digital converter, and in digital form, the controller rescales the amount of analog-to-digital output to obtain the actual amount of current. So, current scaling errors are inevitable [16]. Assuming ideal current tracking, the measured phase currents will be equal to:

$$i_{as} = I \cos\left(\theta_s - \frac{2\pi}{3}\right) / k_s \quad (11)$$

$$i_{bs} = I \cos \theta_s / k_s$$

Based on the similar analysis, current offset error  $\Delta i_{qs}$  can be calculated as follow:

$$\Delta i_{qs} = i_{qz-AD} - i_{qz} = \left(\frac{K_a - K_b}{K_a K_b}\right) \frac{I}{\sqrt{3}} \left[ \cos\left(\theta_s + \frac{2\pi}{3}\right) + \frac{1}{2} \right] \quad (12)$$

From Equations (10) and (12), the torque error is calculated as follows:

$$\Delta T_{m,2} = \left(\frac{K_a - K_b}{K_a K_b}\right) \frac{I}{\sqrt{3}} \left[ \cos\left(\theta_s + \frac{2\pi}{3}\right) + \frac{1}{2} \right] \quad (13)$$

Equation (13) shows that the scaling error causes the torque to fluctuate at twice the fundamental frequency. These analyses show that the electromagnetic torque consists of a DC torque component with harmonic order of 1<sup>st</sup>, 2<sup>nd</sup>, 6<sup>th</sup> and 12<sup>th</sup>. The purpose of the control is to indirectly reduce the torque harmonic waves by the proposed ILC scheme.

### D) Speed ripple due to pulsating torque

According to the following equation, the plant transfer function between the motor speed and the torque will be equal to:

$$\omega_m(s) = \frac{T_m(s) - T_i(s)}{Js + B} \quad (14)$$

As can be seen, the speed fluctuation is the same as the torque fluctuation  $\Delta T_m$ . At low speed it is necessary to minimize torque oscillation sources to minimize speed fluctuations. However, to reduce torque ripple, it is necessary to measure or estimate instantaneous torque, which can make the drive system expensive (by using a torque transducer) or complicated (by using torque observer). Therefore, in the proposed scheme, as described in the next section, the speed data which are already available for the purpose of closed loop speed control is indirectly used to reduce torque ripple. As a result, the reduction in torque fluctuation leads to a reduction in speed ripple.

## 4. Iterative Learning Control for BLDC

Iterative Learning Control (ILC) is a method of tracking control for systems that work in a repetitive mode. This method is useful in dealing with uncertainty of modeling or nonlinearity of the system in response to periodic disturbances in inputs which the system must be able to follow different types of inputs. ILC is actually an error correction algorithm and a memory that stores the previous output data and error information.

### E) ILC Controller Implemented in Time Domain

In the proposed scheme, a P-type learning controller is used, which uses a combined scheme of previous cycle feedback (PCF) and current cycle

feedback (CCF). The implementation of the P-type algorithm is simple and, unlike in the D-type since differentiation of the speed signal is unnecessary, hence noise build-up in input update caused by the differentiation of speed signal can be avoided. In [17], a mathematically rigorous treatment of the robustness and convergence of the P-type learning control algorithm is given. It is showed that the introduction of a forgetting factor  $\alpha$  increases the robustness of the P-type algorithm against noise, initialization error and fluctuation of system dynamics. The proposed ILC scheme in time domain is shown in Fig. 1 and the following learning rule is used:

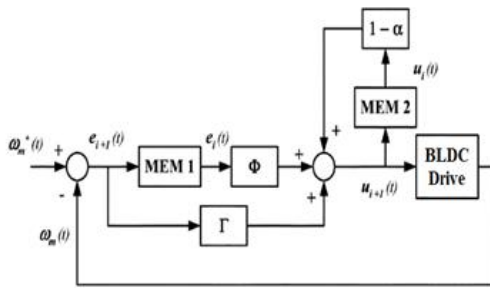


Fig. 1. Block diagram of the ILC scheme implemented in the time domain

$$u_{i+1}(t) = (1-\alpha)u_i(t) + \phi_{\epsilon i}^*(t) + \Gamma_{\epsilon i+1} \tag{15}$$

where  $i = 1, 2, 3, 4, 5, \dots$  shows the iteration number and the control signal of  $u(t)$  is actually the compensated current of the q-axis generated by the ILC.  $e_i(t)$  is the speed error signal that is equal to  $\omega_m^* - \omega_m$ .  $\alpha$  is the forgetting factor; and  $\phi$  and  $\Gamma$  are the PCF and CCF gains, respectively. Assuming perfect tracking of the inner-loop of the current controller, the learning gain can be calculated as follow:

$$T_m(t) = T_m^*(t) = k_t i_{qs}^*(t) \tag{16}$$

By substituting (16) into (4), equation (17) is obtained:

$$\frac{d\omega_m}{dt} = -\frac{B}{J}\omega_m + \frac{k_t}{J}i_{qs} - \frac{T_l}{J} \tag{17}$$

For the convergence purposes, the following conditions must be met [18]:

$$\|1 - \frac{k_t}{J}\phi\| < 1 \tag{18}$$

Given, the inequality of (18) can be solved as (19):

$$0 < \phi < \frac{2}{\left| \frac{k_t}{J} \right| m \alpha} \tag{19}$$

By knowing the range of d-axis flux linkage  $\Psi_{dm}$  and the total inertia of  $J$ , the learning gain  $\phi$  can be determined. To achieve a faster rate of convergence, the gain value  $\phi$  should approach. Nevertheless, a conservative choice that guarantees stability and rapid convergence is sufficient. Theoretically the value of CCF ( $\Gamma$ ) does not affect the convergence in the iteration axis of the learning controller [16]. However, too much  $\Gamma$  causes the error or noise signals in the input to increase too much, and the output of the controller tends to increase in value, leading to divergence and instability of the output.

F) Implementation of Drive System

Fig. (2) shows the outline of the utilized drive to reduce speed ripple. In the transient state, the ILC is disabled and  $i_{qs}^*$  is provided only by the output of the PI speed controller. By reaching the steady state, the ILC compensator signal ( $\Delta i_{qs}^*$ ) is added to  $i_{qs}^*$  so as to minimize speed ripples. To evaluate the ILC controller, the performance of the drive system by applying the ILC controller is compared with the only PI controller.

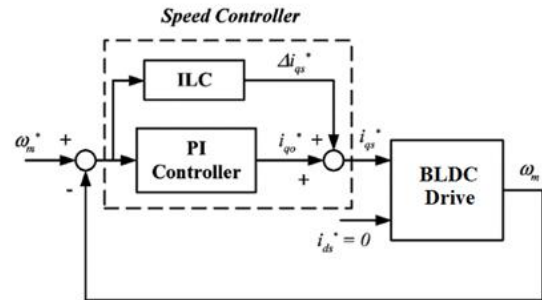


Fig. 2. Speed control loop block diagram used in BLDC drive system

5. Simulations

Various operational scenarios have been performed to evaluate the effectiveness of the proposed the ILC scheme. In this case, the motor speed is set to 0.2 p.u. and the range of load torque is changed from zero to 2 Nm. The performance criterion for evaluating the efficiency of the proposed scheme for reducing speed ripple is the speed ripple factor (SRF). the proposed scheme is modeled in Matlab/Simulink. The values of the BLDC model parameters are listed in Table 1. The

SRF coefficient is the ratio of peak-to-peak speed ripple to the nominal speed of BLDC motor:

$$SRF = \frac{\omega_{pk} - \omega_{vk}}{\omega_{nom}} \times 100\% \quad (20)$$

Table.1.  
BLDC motor parameters

| Value                 | Symbol             | Parameters        |
|-----------------------|--------------------|-------------------|
| 1.64 kW               | $P_{nominal}$      | Rated Power       |
| 2000 rpm              | $\omega_{nominal}$ | Rated Speed       |
| 2.125 $\Omega$        | $R_s$              | Stator resistance |
| 11.6 mH               | $L_s$              | Stator Inductance |
| 0.387 Wb              | $\phi$             | Magnet Flux       |
| 6                     | $P$                | Number of poles   |
| 0.3 kg.m <sup>2</sup> | $J$                | Inertia           |

The SRF of the BLDC drive is first determined using a standard PI speed controller alone. The proposed ILC controller that generates the compensation current is then applied in parallel and the corresponding SRF is re-evaluated. Fig. 3 shows the speed response for different operating modes at the speed of 0.2 p.u. (400 rpm). Fig. (3-a) presents the motor speed response without external load torque and without ILC compensator. In this operating mode, the speed fluctuation of 10% is determined according to Fig. (3-a) and the SRF coefficient. In order to evaluate the efficiency of the ILC compensator, the speed waveform with adding this compensator is plotted in Fig. (3-b). According to this figure, the reduction of the speed ripple in this working mode is evident by adding the proposed controller. The speed ripple has reduced to about 4% with the applying the proposed controller. Also, by increasing the load torque by 2 N.m, the performance of the proposed controller is investigated. By comparing Fig. (3-c) and (3-d) which show the motor speed at the torque of 2 N.m without and with the ILC compensator respectively, a 5% reduction in speed ripple is determined. In order to further evaluate the effectiveness of the proposed controller, the frequency response has been investigated. According to Fig. (4-a) to (4-d), with the addition of the ILC compensator, the value of total harmonic distortion (THD) has significantly reduced. These values are listed in Table 2. The results show that this compensator well eliminates the 6<sup>th</sup> and 12<sup>th</sup> order speed wave harmonics and generates a more uniform speed waveform.

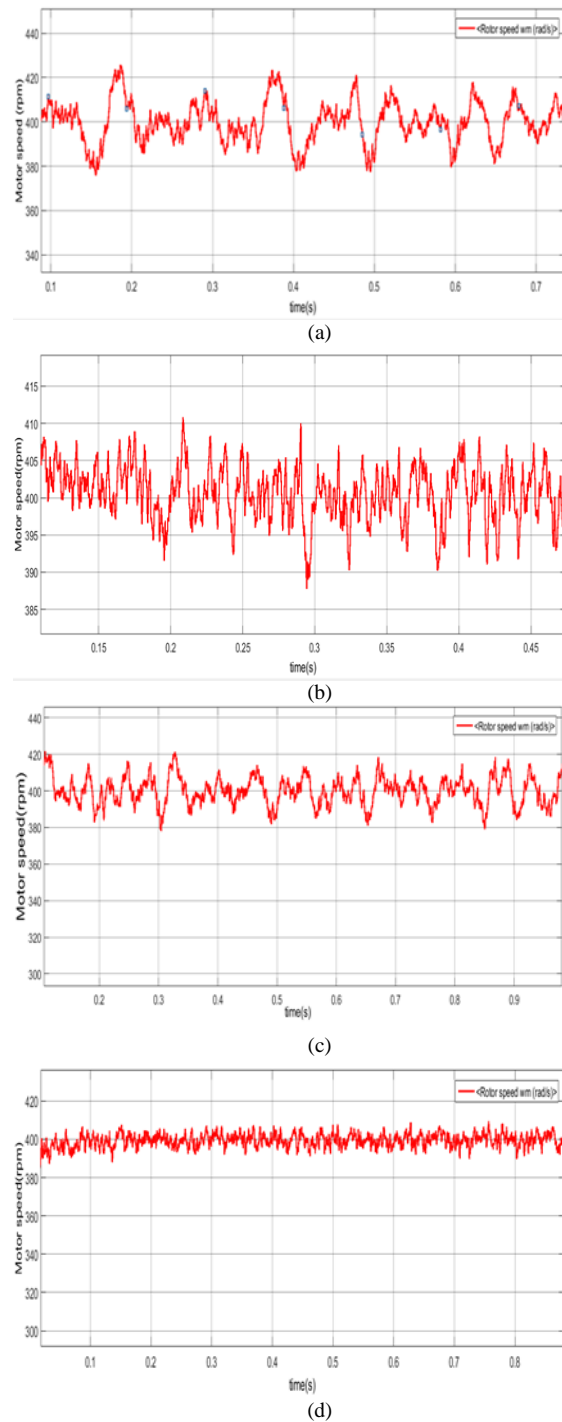
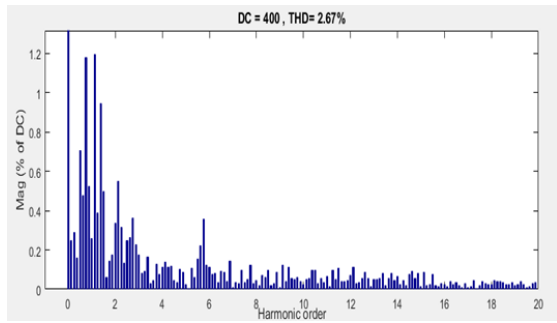
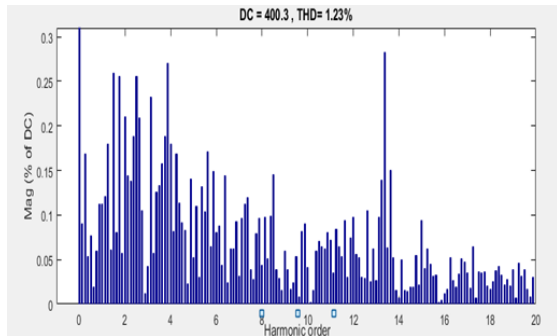


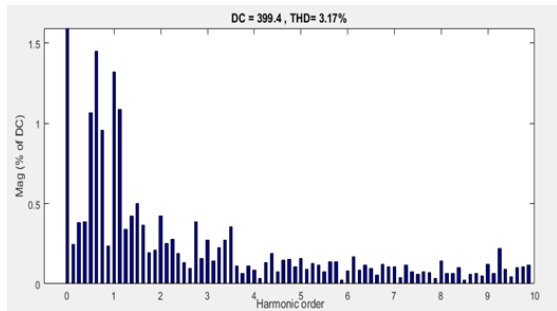
Fig. 3. Motor speed response in different operating modes; (a) without ILC compensator at zero torque, (b) with ILC compensator at zero torque, (c) without ILC compensator at 2 N.m torque, and (d) with ILC compensator at 2 N.m torque



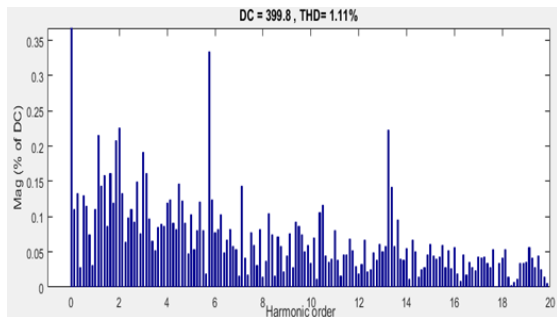
(a)



(b)



(c)



(d)

Fig. 4. Frequency response of motor speed waveform in different operating modes; (a) without ILC compensator at zero torque, (b) with ILC compensator at zero torque, (c) without ILC compensator at 2 N.m torque, and (d) with ILC compensator at 2 N.m torque

Table.2.

Comparison of speed ripple and speed distortion before and after adding the proposed compensator at 400 rpm

| $T_l(N.m)$ | Parameters                      | With ILC | Without ILC |
|------------|---------------------------------|----------|-------------|
| 0          | Speed ripple factor (SRF)       | 4%       | 10%         |
| 0          | Total harmonic distortion (THD) | 1.23%    | 2.67%       |
| 2          | Speed ripple factor (SRF)       | 5.01%    | 10.03%      |
| 2          | Total harmonic distortion (THD) | 1.11%    | 3.17%       |

According to Table 2, with increasing load torque, the amount of SRF has increased as with increasing load, the motor coupling is affected by torque fluctuations that the ILC compensator is not able to eliminate and as a result, an increase in SRF is observed.

In addition to reducing the speed ripple, applying this compensator causes the over-shoot of the speed waveform to be well eliminated, which eliminates the need for soft-starter and ultimately increases the response speed of the drive. According to Fig. 5 and 6, by adding the ILC compensator, the amount of over-shoot of the BLDC motor speed is reduced from 35% to zero, which shows the effectiveness of the proposed controller.

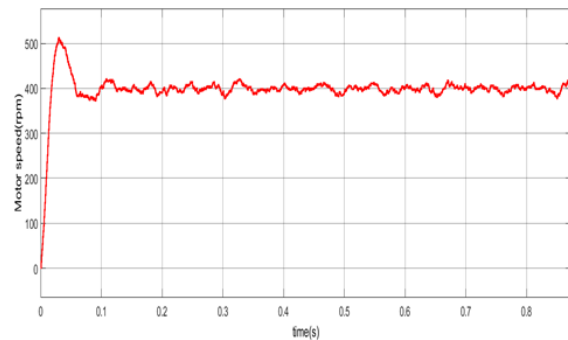


Fig. 5. motor speed over-shoot without ILC compensator at the torque 2 N.m and speed of 400 rpm

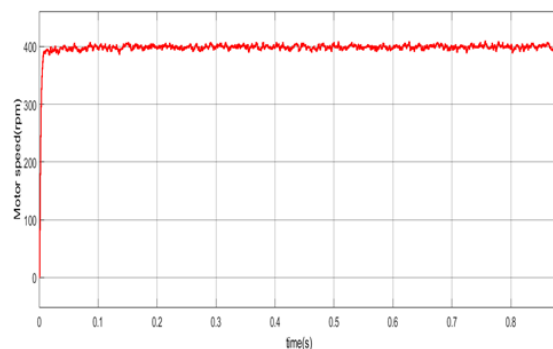


Fig. 6. motor speed over-shoot with ILC compensator at the torque 2 N.m and speed of 400 rpm

## 6. Conclusion

In this paper, a proposed controller are introduced and investigated to reduce the speed ripple. Due to the nature of torque and speed cycles, learning control is an efficient and appropriate choice to reduce speed ripple. In order to evaluate the efficiency of adding ILC controller to BLDC motor drive, simulation of motor drive system was performed in Matlab/Simulink and the results showed that this method can lead to a reduction of ripple speed. By defining the speed ripple factor (SRF), improvement and decrease in speed ripple were observed in different motor operating scenarios, and according to the frequency response of the motor speed, the addition of the proposed controller can effectively reduce the harmonic orders of the 6<sup>th</sup> and 12<sup>th</sup>. By investigating the motor speed waveform at start-up, a significant reduction in the over-shoot of motor speed was observed by adding the ILC controller, which this in turn increases the response speed of the drive. The proposed controller can be added to any existing controller and does not require accurate knowledge of motor parameters. Therefore, it is a practical solution to improve the efficiency of using BLDC motors, especially in servomotor applications, including servomotors used in aircraft flaps. Having smooth handling and high accuracy along with proper response speed in the servo motor of aircraft flap is a necessity that the proposed controller in this research, can well achieve to it.

## References

- [1] N. V. Nguyen et al, "Flap Design Optimization for Very Light Aircraft in compliance with Airworthiness Certification," Computational Fluid Dynamics Conference, June 24-27, 2013, San Diego, CA.
- [2] T. M. Jahns, and W. L. Soong, "Pulsating torque minimization techniques for permanent magnet ac drives—A review," IEEE Trans. Ind. Electron., vol. 43, no. 2, pp. 321–330, Apr. 1996.
- [3] C. Studer, A. Keyhani, T. Sebastian, and S. K. Murthy, "Study of cogging torque in permanent magnet machines," in Proc. IEEE 32nd Ind. Appl. Society (IAS) Annu. Meeting, vol. 1, New Orleans, LA, Oct. pp. 42–49, 1997.
- [4] J. Y. Hung and Z. Ding, "Design of currents to reduce torque ripple in brushless permanent magnet motors," Proc. Inst. Elect. Eng. B, vol. 140, no. 4, pp. 260–266, 1993.
- [5] D. C. Hanselman, "Minimum torque ripple, maximum efficiency excitation of brushless permanent magnet motors," IEEE Trans. Ind. Electron., vol. 41, no. 3, pp. 292–300, Jun. 1994.
- [6] J. Holtz and L. Springob, "Identification and compensation of torque ripple in high-precision permanent magnet motor drives (invited paper)," IEEE Trans. Ind. Electron., vol. 43, no. 2, pp. 309–320, Apr. 1996.
- [7] V. Petrovic, R. Ortega, A. M. Stankovic, and G. Tadmor, "Design and implementation of an adaptive controller for torque ripple minimization in PM synchronous motors," IEEE Trans. Power Electron., vol. 15, no. 5, pp. 871–880, Sep. 2000.
- [8] T. S. Low, T. H. Lee, K. J. Tseng, and K. S. Lock, "Servo performance of a BLDC drive with instantaneous torque control,"

IEEE Trans. Ind. Appl., vol. 28, no. 2, pp. 455–462, Mar./Apr. 1992.

[9] N. Matsui, T. Makino, and H. Satoh, "Auto compensation of torque ripple of direct drive motor by torque observer," IEEE Trans. Ind. Appl., vol. 29, no. 1, pp. 187–194, Jan./Feb. 1993.

[10] S. K. Chung, H. S. Kim, C. G. Kim, and M.-J. Youn, "A new instantaneous torque control of PM synchronous motor for high-performance direct-drive applications," IEEE Trans. Power Electron., vol. 13, no. 3, pp. 388–400, May 1998.

[11] F. Colamartino, C. Marchand, and A. Razek, "Torque ripple minimization in permanent magnet synchronous servodrive," IEEE Trans. Energy Conversion, vol. 14, no. 3, pp. 616–621, Sep. 1999.

[12] Liu, J., Li, H. and Deng, Y., "Torque ripple minimization of PMSM based on robust ILC via adaptive sliding mode control. IEEE Transactions on Power Electronics, 33(4), pp.3655-3671, 2017.

[13] Liu, Q. and Hameyer, K., "Torque ripple minimization for direct torque control of PMSM with modified FCSMPC. IEEE Transactions on Industry Applications, 52(6), pp.4855-4864, 2016.

[14] Sumega, M., Zossak, S., Varecha, P., Rafajdus, P. and Stulrajter, M., "Adaptive algorithm to reduce acoustic noise and torque ripple in low-cost PM motors." In 2019 International Aegean Conference on Electrical Machines and Power Electronics (ACEMP) & 2019 International Conference on Optimization of Electrical and Electronic Equipment (OPTIM) (pp. 100-107). IEEE.

[15] Fei, Q., Deng, Y., Li, H., Liu, J. and Shao, M., "Speed ripple minimization of permanent magnet synchronous motor based on model predictive and iterative learning controls." IEEE Access, vol. 7, pp.31791-31800, 2019.

[16] D.W. Chung and S. K. Sul, "Analysis and compensation of current measurement error in vector-controlled ac motor drives," IEEE Trans. Ind. Appl., vol. 34, no. 2, pp. 340–345, Mar./Apr. 1998.

[17] S. Arimoto, T. Naniwa, and H. Suzuki, "Robustness of P-type learning control with a forgetting factor for robotic motions," in Proc. 1990 IEEE Decision and Control Conf., vol. 5, Dec. 5–7, pp. 2640–2645.

[18] Z. Bien and J.-X. Xu, Iterative Learning Control—Analysis, Design, Integration, and Applications. Boston, MA: Kluwer, 1998.